ISSN: 1692-7257 - Volume 2 – Issue 48 - 2026

ORIGINAL

RCTA
Revista Colombiana de Tecnologías de Avanzada
UNIPAMPLONA

Site-Specific Modeling of Continuous Electromagnetic Field Exposure in Bogotá

Modelación específica por sitio de la exposición continua a campos electromagnéticos en Bogotá

Osnamir Elias Bru-Cordero[1]
Juan Guillermo Popayán Hernández[1]
Cristian David Correa Álvarez[2]

[1] **Universidad Nacional de Colombia, Sede De La Paz, Dirección Académica, La Paz, Cesar, Colombia.**
[2] **Universidad Nacional de Colombia, Sede Manizales, Departamento de Matemáticas y Estadística, Manizales, Colombia.**

Received: 17 April 2026. Revised: 25 June 2026. Accepted: 24 July 2026. Published: 27 July 2026.
Corresponding Author: Osnamir Elias Bru-Cordero

How to cite: O. Elias Bru-Cordero, J. G. Popayán Hernández, and C. D. Correa Álvarez, "Modelación específica por sitio de la exposición continua a campos electromagnéticos en Bogotá", *Revista Colombiana de Tecnologías de Avanzada (RCTA)*, vol. 2, no. 48, jul. 2026, art. no. 4411, doi: 10.24054/rcta.v2i48.4411

This work is licensed under a Creative Commons Attribution-NonCommercial 4.0 International License.

Abstract:

This study develops and validates a reproducible, site-sensitive workflow for analyzing continuous electromagnetic field monitoring data published as open data by the National Spectrum Agency (ANE) of Colombia. The Bogotá subset contains 481,148 broadband electric field measurements averaged over six-minute intervals, collected by nine fixed probes between November 2, 2023, and June 30, 2024. After harmonizing timestamps and applying a completeness filter, 2,009 probe-day records were analyzed. To account for the longitudinal structure of the dataset, two ordinary least squares log-linear specifications with HC3 robust inference were compared with a random-intercept mixed-effects model, and an additional model was estimated for the daily 95th percentile. The temporal-only model explained little variation in mean daily exposure (adjusted $R^2 = 0.007$), whereas the model with probe fixed effects captured most of the variability (adjusted $R^2 = 0.964$). The mixed-effects model led to the same interpretation (marginal $R^2 = 0.016$; conditional $R^2 = 0.964$), while the p95 model retained a strongly site-dependent structure (adjusted $R^2 = 0.951$). Regression diagnostics indicated non-normality, heteroscedasticity, and positive residual autocorrelation, but no high-leverage observations or influential observation capable of explaining the high model fit were identified. The maximum six-minute field observed was 0.21011 V/m, below 1% of the public contextual reference value of 28 V/m. The differential contribution of this study is not to make a general claim that site conditions matter, but rather to validate this structure specifically for Bogotá through an auditable open-data workflow that reports complete coefficients, diagnostics, and robustness in the upper tail.

Keywords: Electromagnetic field monitoring; Bogotá; open data; fixed-effects modeling; mixed-effects models; regression diagnostics; telecommunications infrastructure.

Resumen:

Este estudio desarrolla y valida un flujo de trabajo reproducible y sensible al sitio para analizar datos continuos de monitoreo de campos electromagnéticos publicados como datos abiertos por la Agencia Nacional del Espectro (ANE) de Colombia. El subconjunto de Bogotá contiene 481.148 mediciones de campo eléctrico de banda ancha promediadas cada seis minutos, recolectadas por nueve sondas fijas entre el 2 de noviembre de 2023 y el 30 de junio de 2024. Tras armonizar las marcas de tiempo y aplicar un filtro de completitud, se analizaron 2.009 registros sonda-día. Para atender la estructura longitudinal del archivo, se compararon dos especificaciones log-lineales de mínimos cuadrados ordinarios con inferencia robusta HC3 con un modelo mixto de intercepto aleatorio, y además se estimó un modelo complementario para el percentil 95 diario. El modelo solo temporal explicó poca variación en la exposición media diaria (R^2 ajustado = 0,007), mientras que el modelo con efectos fijos por sonda capturó la mayor parte de la variabilidad (R^2 ajustado = 0,964). El modelo mixto condujo a la misma interpretación (R^2 marginal = 0,016; R^2 condicional = 0,964), y el modelo p95 conservó una estructura fuertemente dependiente del sitio (R^2 ajustado = 0,951). Los diagnósticos de regresión mostraron no normalidad, heterocedasticidad y autocorrelación residual positiva, pero no observaciones con leverage alto ni una observación influyente capaz de explicar el alto ajuste. El campo máximo observado en seis minutos fue 0,21011 V/m, por debajo del 1% de la referencia contextual pública de 28 V/m. La contribución diferencial del estudio no es afirmar de forma general que las condiciones del sitio importan, sino validar esta estructura de manera específica para Bogotá mediante un flujo auditable de datos abiertos que reporta coeficientes completos, diagnósticos y robustez en la cola superior.

Palabras clave: Monitoreo de campos electromagnéticos; Bogotá; datos abiertos; modelación con efectos fijos; modelos mixtos; diagnósticos de regresión; infraestructura de telecomunicaciones.

INTRODUCTION

Exposure to electromagnetic fields (EMF) from wireless communication systems remains a technical and regulatory issue, because telecommunications infrastructure continues to expand while spectrum authorities require transparent evidence on public radiofrequency conditions. The World Health Organization frames EMF exposure as both an engineering and a communication challenge, and the long-term monitoring approach formalized in ITU-T Recommendation K.83 was created to support that need [1]–[3].

In Colombia, this monitoring logic is reflected in the regulatory framework on non-ionizing radiation and in the open data publication strategy of the National Spectrum Agency (ANE), which releases continuous records from its electromagnetic field monitoring system[4],[5]. The engineering implication is that exposure assessment is no longer limited to isolated field campaigns; it is also part of infrastructure oversight, spectrum governance and technical accountability.

The international literature shows that continuous monitoring has become established as a practical tool for engineering interpretation and public communication. Reviews on EMF monitoring concepts, measurement instruments and exposure patterns in microenvironments have documented the value of broadband observations for characterizing low levels of public exposure and comparing monitoring strategies across contexts [7]–[9]. Continuous observatories in Greece and other countries further show that long-term fixed measurements make it possible to identify stable exposure patterns, seasonal modulation and persistent differences between sites, while remaining below public reference levels [10]–[12].

A second line of the literature emphasizes that radiofrequency exposure patterns are determined by local site conditions rather than by time in isolation. Studies around base stations, urban wireless systems and residential areas have repeatedly found that measured levels depend on transmitter geometry, urban form, network density and the composition of active services [13]–[15]. Modeling studies have extended this idea through geospatial, surrogate and spatiotemporal approaches, showing that exposure data are most useful for engineering decisions when they are converted into interpretable statistical models and not merely into isolated measurements [16]–[20]. Recent work on long-term monitoring, small cells and 5G environments confirms that temporal variation exists, but that the strongest structure usually depends on the site[12], [23]–[25].

The scientific gap addressed here is therefore more specific than the general observation that sites differ. For Latin American open data datasets, there are still few reproducible studies that audit the semantics of public monitoring variables, separate site baselines from calendar effects within the same metropolitan environment, report complete model outputs, and verify whether the same conclusion holds for routine exposure and for upper-tail indicators such as the 95th percentile. This gap matters because a national open data release mixes cities, probes and operational histories; without a site-sensitive workflow and diagnostics, public data can be summarized but not fully interpreted for local engineering decisions.

This article therefore develops a Bogotá-specific statistical analysis of the ANE continuous monitoring dataset. The objectives are to characterize the Bogotá subset after transparent preprocessing, to compare a time-only specification with a probe fixed effects model for mean daily electric field intensity, to evaluate regression diagnostics and longitudinal robustness by means of a mixed model, and to verify whether a complementary p95 model supports the same interpretation. The distinctive contribution is an auditable workflow that turns a Colombian open monitoring dataset into site-level interpretable evidence for baselines, anomaly detection and public technical communication.

MATERIALS AND METHODS

Open dataset and analytical scope for Bogotá

The raw data come from the open government repository “Mediciones de exposición a campos electromagnéticos” maintained by the ANE[5]. The national CSV dataset contains the fields Ubicacion_Sonda, Ciudad_Departamento, Fecha_Medicion, Nivel_Exposicion, Limite_Restrictivo, Porcentaje_Exposicion and Punto_Georreferenciado.

In its released form, the dataset contains 1,286,346 six-minute intervals obtained by 26 probes distributed across 12 city-department labels. The present study restricted the analysis to the Bogotá subset because it contains the largest number of probes within a common metropolitan environment and is therefore more suitable for assessing site-specific behavior without mixing it with differences between cities.

After filtering by probe identifier, the Bogotá subset contains 481,148 six-minute broadband electric field records, collected by nine fixed probes between November 2, 2023, and June 30, 2024. The analytical variable of interest was Nivel_Exposicion, defined in the ANE technical documentation as RMS electric field intensity in V/m, measured by broadband isotropic equipment under the long-duration logic of ITU-T K.83[3],[5].

The current CSV dataset includes Limite_Restrictivo and Porcentaje_Exposicion, but these variables were not used as inferential modeling targets because the dataset encodes a constant restrictive value of 2, whereas the archived supporting document describes a contextual public reference of 28 V/m for the published set[4],[5]. To avoid propagating undocumented

transformations, all inferential analysis was based on the field intensity measured directly in V/m. Percentages relative to 28 V/m were retained only for contextual descriptive reporting.

Preprocessing and descriptive indicators

Timestamp preprocessing converted Fecha_Medicion into valid calendar dates and times using the format “Y b d I:M:S p”; the data were then aggregated by probe and calendar day. For each probe-day, the pipeline calculated the number of valid six-minute intervals, the daily mean field, the daily median, the daily 95th percentile and the daily maximum. Because the monitoring logic is based on six-minute averages, a nominal full day contains 240 observations. To ensure comparable daily windows, the analysis retained only probe-days with at least 200 valid records.

The resulting analytical sample contains 2,009 retained probe-day records, with an average of 239.1 six-minute measurements per retained day. Month and day of the week were derived from the calendar date. Unlike the previous version of the manuscript, the daily p95 was not left solely as a descriptive indicator: it was retained in the descriptive characterization and was also modeled as an upper-tail robustness target to verify whether the mean-based interpretation held for high routine exposure.

Statistical models, longitudinal rationale and diagnostics

Two complementary log-linear models were estimated for the daily mean electric-field intensity. Model A assessed calendar effects only, whereas Model B added probe fixed effects to capture persistent site heterogeneity. The logarithmic transformation was used because daily field values were positive, right-skewed and easier to interpret multiplicatively after exponentiating the coefficients.

$$\log(\text{MeanE_pd} + 10^{-6}) = \beta 0 + \gamma m + \delta w + \varepsilon pd. \quad (1)$$

$$\log(\text{MeanE_pd} + 10^{-6}) = \beta 0 + \alpha p + \gamma m + \delta w + \varepsilon pd. \quad (2)$$

In Equations (1) and(2), p denotes the probe, d the calendar day, m the month and w the day of the week. The term αp represents the probe-specific fixed effect, γm the monthly effect, δw the day-of-the-week effect and εpd the unexplained component. Ordinary least squares was retained as the main estimator because the purpose was to estimate fixed, interpretable baselines within the observed monitoring network, not to predict unobserved probes. This fixed-effects formulation is a standard strategy for panel-type data when the aim is to remove time-invariant heterogeneity[26],[27].

To address the longitudinal nature of the data, Model B was not treated as the only evidence. A random-intercept mixed-effects model was estimated, log(MeanEpd + 10^-6) = β0 + up + γm + δw + εpd, where up represents a probe-level random intercept, as a panel-sensitive robustness check. The mixed model tests whether the same site-dominated interpretation emerges when the probe structure is represented as a random effect rather than as a fixed set of site indicators[26].

The observation on p95 raised in the review was addressed by estimating a third model with the same predictors as Model B, but replacing the response with log(p95Epd + 10^-6). This model does not replace the daily mean specification; it verifies whether the upper tail of routine exposure follows the same site and calendar structure.

$$\log(\text{p95E_pd} + 10^{-6}) = \beta 0 + \alpha p + \gamma m + \delta w + \varepsilon pd. \quad (3)$$

Coefficient inference for the OLS models used HC3 robust covariance matrices to address heteroscedasticity. The full coefficient tables report estimates, robust standard errors, 95% confidence intervals, p-values and exponentiated effects. Model adequacy was assessed using residual normality tests, heteroscedasticity tests, residual-versus-fitted plots, Q-Q plots, studentized residuals, leverage, Cook’s distance, pooled Durbin-Watson values and lag 1 residual autocorrelation per probe. These diagnostics are used to qualify the inference and not to conceal model limitations[28].

Reproducibility framework

The revised workflow was programmed in R [22] using readr, dplyr, lubridate, ggplot2, sandwich, lmtest, broom, tidyr, forcats and nlme. The updated script automates data import, date processing, Bogotá filtering, probe-day aggregation, the completeness filter, descriptive summaries, model estimation, HC3 inference, export of full coefficients, p95 modeling, robustness with mixed-effects models, diagnostic tables, diagnostic figures and export of session information. This reproducible structure matters not only for transparency but also because the open dataset requires semantic auditing before variables derived from the limit can be interpreted.

Availability of materials and data

The raw monitoring data are publicly available on the Colombian open data portal maintained by the National Spectrum Agency [5]. The revised R workflow specific to Bogotá generates the derived probe-day dataset, the full coefficient tables, the diagnostics, the figures and the reproducibility metadata that accompany this manuscript.

RESULTS AND DISCUSSION

Descriptive characterization of the Bogotá monitoring dataset

Table 1 summarizes the analytical subset of Bogotá obtained after the entire preprocessing sequence. The city-specific file retained 481,148 six-minute broadband records and 2,009 nearly complete day-to-day probe observations from nine monitoring probes. The observation window extended from November 2, 2023, to June 30, 2024, and the average retained probe day contains 239.1 valid six-minute measurements. The overall mean daily field average was 0.02679 V/m, while the overall daily p95 average was 0.03791 V/m.

The maximum six-minute field observed in the Bogotá subset was 0.21011 V/m, below 1% of the contextual public reference of 28 V/m described in the archived ANE supporting document[4],[5]. This magnitude is consistent with continuous monitoring studies that report low levels of public exposure even in dense urban environments[10],[15],[21].

Table 1: Summary of the Bogotá analytical subset.

Metric	Value
Raw six-minute records in Bogotá	481,148
Retained probe-day records	2,009
Different probes in Bogotá	9
Observation period	2023-11-02 to 2024-06-30
Average number of six-minute intervals recorded per retained day	239.1
Overall mean of the daily mean E (V/m)	0.02679
Overall median of the daily mean E (V/m)	0.01060
Overall mean of the daily p95 of E (V/m)	0.03791
Maximum field observed in six-minute intervals (V/m)	0.21011
Maximum daily mean as % of 28 V/m	0.49
Maximum daily p95 as % of 28 V/m	0.60

Source: author's own elaboration based on ANE open data. The values relative to 28 V/m are contextual descriptors, not inferential objectives.

The strongest descriptive feature of the Bogotá subset is the heterogeneity among probes. Table 2 and Fig. 1 show that Bogota_AEROCIVIL had the highest daily mean field (0.12759 V/m), followed by Bogota_ANE_2 (0.04944 V/m), whereas Bogota_TES_1 averaged only 0.00243 V/m. This represents a difference of more than fifty times between the probe with the highest and the one with the lowest average.

Table 2: Ranking of Bogotá probes according to the mean daily electric field level.

Probe	Days	Daily mean E	Mean daily p95	Maximum observed E	Mean % of 28 V/m
Bogota_AEROCIVIL	242	0.12759	0.15116	0.21011	0.456
Bogota_ANE_2	199	0.04944	0.08642	0.15932	0.177
Bogota_MINTIC	242	0.01679	0.03176	0.12665	0.06
Bogota_BATALLON_BARAYA	207	0.01144	0.01746	0.02435	0.041
Bogota_CAN_CGFM	209	0.01115	0.01699	0.02819	0.04
Bogota_AEROPUERTO_GUAYMARAL	242	0.0091	0.01757	0.02941	0.032
Bogota_ANE	234	0.00386	0.00734	0.03495	0.014
Bogota_BATALLON_USME	208	0.00332	0.00398	0.00749	0.012
Bogota_TES_1	226	0.00243	0.00328	0.00629	0.009

Source: author's own elaboration. Mean percentages are relative to 28 V/m.

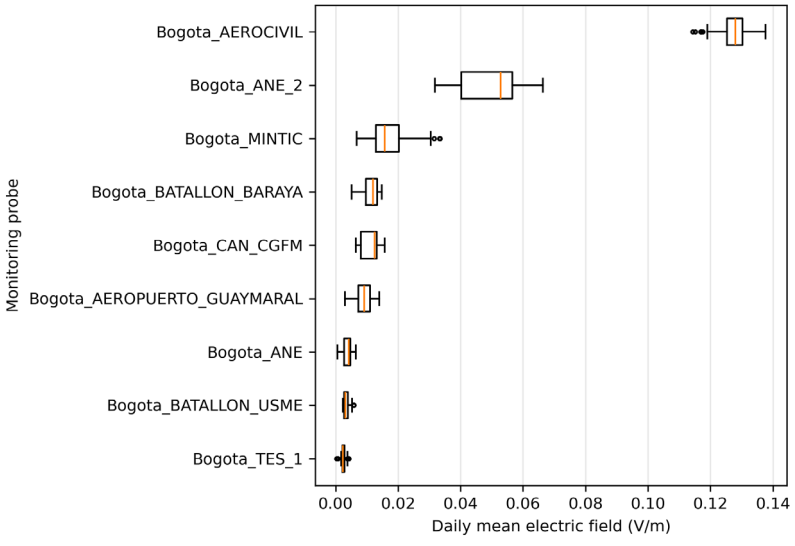

Fig. 1. *Distribution of the mean daily electric field among monitoring probes in Bogotá.*
Source: author's own elaboration.

The raw temporal profiles are informative, but they must be interpreted with caution because the unequal availability of probes may confound temporal effects with site composition. Monthly averages show moderate variation in both the mean daily value and the daily p95, whereas averages by day of the week show lower levels on Saturdays and Sundays than from Tuesday to Friday. These patterns motivated the adjusted models presented below.

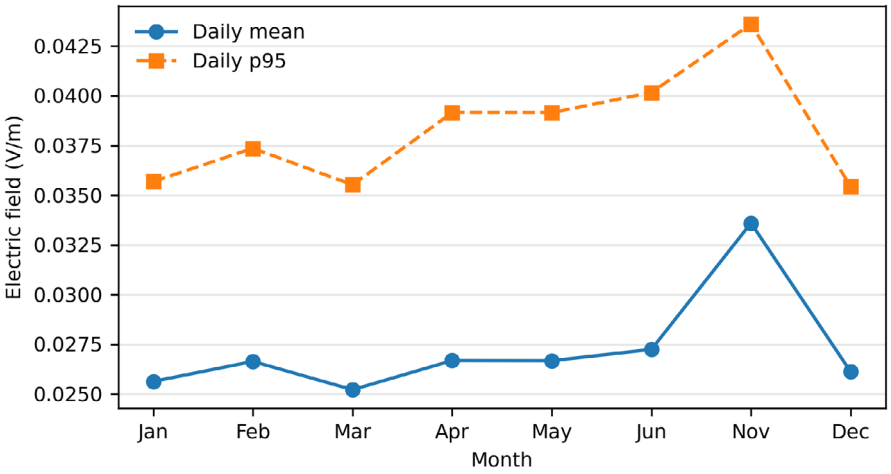

Fig. 2. *Monthly averages of the mean daily value and the daily p95 of the electric field in Bogotá. Source: author's own elaboration.*

Temporal-only modeling versus probe-adjusted modeling

Table 3 compares the mean daily models and the complementary p95 model. Model A, which included only month and day-of-week terms, explained almost no variability in mean daily exposure (adjusted $R^2 = 0.007$). Model B, which added probe fixed effects, substantially changed the result: the adjusted R^2 increased to 0.964 and the residual standard error fell from 1.270 to 0.242 on the logarithmic scale. The contrast between the two specifications is the central empirical result of the article. In Bogotá, the broad calendar structure is not sufficient to characterize the mean daily field intensity; most of the explainable variability is linked to the monitoring site.

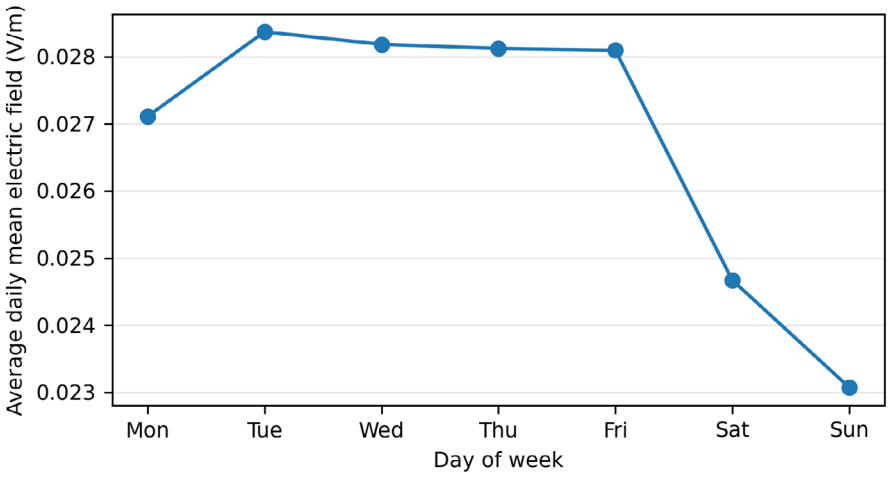

Fig. 3. *Averages by day of the week of the mean daily electric field in Bogotá. Source: author's own elaboration.*

Table 3: Comparison of log-linear models based on the mean and p95.

Model	Target variable	N	Adjusted R^2	AIC (R style)	Residual standard error
A: month + day of the week	Daily mean of E	2009	0.007	6678.6	1.270
B: month + day of the week + probe fixed effects	Daily mean of E	2009	0.964	25.9	0.242
C: upper tail model p95 (month + day + probe)	Daily p95 of E	2009	0.951	640.6	0.282

AIC values follow the R lm convention used by the updated script. Source: author's own elaboration.

Tables 4A and 4B present the complete coefficient output requested during the review. Coefficients are reported on the

logarithmic scale. Exp(beta) corresponds to the multiplicative factor relative to the reference category. In Model B, the reference profile is Bogota_AEROCIVIL in January and Monday.

Table 4A: Complete table of HC3 coefficients for Model A: log daily mean of E ~ month + day of the week.

Term	Estimate	HC3 SE	IC 95%	p	Exp(beta)
Intercept / reference	-4.485	0.101	[-4.683, -4.287]	<0.001	0.011
Month: Feb vs Jan	0.059	0.104	[-0.146, 0.263]	0.574	1.06
Month: Mar vs Jan	-0.003	0.103	[-0.206, 0.200]	0.975	0.997
Month: Apr vs Jan	0.035	0.107	[-0.174, 0.244]	0.741	1.036
Month: May vs Jan	0.025	0.106	[-0.182, 0.232]	0.811	1.026
Month: Jun vs Jan	0.057	0.107	[-0.154, 0.267]	0.597	1.058
Month: Nov vs Jan	-0.158	0.163	[-0.478, 0.161]	0.332	0.854
Month: Dec vs Jan	0.014	0.105	[-0.193, 0.220]	0.897	1.014
Day: Tue vs Mon	0.107	0.107	[-0.103, 0.317]	0.317	1.113
Day: Wed vs Mon	0.095	0.107	[-0.115, 0.305]	0.375	1.1
Day: Thu vs Mon	0.083	0.107	[-0.127, 0.292]	0.439	1.086
Day: Fri vs Mon	0.064	0.107	[-0.146, 0.275]	0.549	1.067
Day: Sat vs Mon	-0.156	0.108	[-0.367, 0.055]	0.148	0.856
Day: Sun vs Mon	-0.282	0.109	[-0.495, -0.070]	0.009	0.754

Reference categories: January and Monday. Abbreviations: Jan, Feb, Mar, Apr, May, Jun, Nov, Dec; Mon, Tue, Wed, Thu, Fri, Sat, Sun. Source: author's own elaboration.

Table 4B: Full table of HC3 coefficients for Model B: log daily mean of E ~ month + day of the week + probe fixed effects.

Term	Estimate	HC3 SE	IC 95%	p	Exp(beta)
Intercept / reference	-2.045	0.022	[-2.089, -2.001]	<0.001	0.129
Month: Feb vs Jan	0.062	0.016	[0.030, 0.094]	<0.001	1.064
Month: Mar vs Jan	0.001	0.018	[-0.035, 0.037]	0.972	1.001
Month: Apr vs Jan	0.039	0.018	[0.003, 0.075]	0.032	1.04
Month: May vs Jan	0.029	0.017	[-0.004, 0.062]	0.084	1.029
Month: Jun vs Jan	0.031	0.018	[-0.003, 0.066]	0.077	1.032
Month: Nov vs Jan	-0.26	0.046	[-0.351, -0.169]	<0.001	0.771
Month: Dec vs Jan	0.041	0.021	[-0.000, 0.081]	0.050	1.041
Day: Tue vs Mon	0.107	0.021	[0.066, 0.149]	<0.001	1.113
Day: Wed vs Mon	0.105	0.021	[0.064, 0.147]	<0.001	1.111
Day: Thu vs Mon	0.095	0.022	[0.052, 0.137]	<0.001	1.099
Day: Fri vs Mon	0.066	0.022	[0.023, 0.109]	0.003	1.068
Day: Sat vs Mon	-0.15	0.022	[-0.193, -0.107]	<0.001	0.861
Day: Sun vs Mon	-0.276	0.024	[-0.323, -0.230]	<0.001	0.759
Probe: Bogota_AEROPUERTO_GUAYMARAL vs Bogota_AEROCIVIL	-2.677	0.019	[-2.715, -2.640]	<0.001	0.069
Probe: Bogota_ANE vs Bogota_AEROCIVIL	-3.549	0.021	[-3.590, -3.508]	<0.001	0.029
Probe: Bogota_ANE_2 vs Bogota_AEROCIVIL	-0.999	0.014	[-1.026, -0.972]	<0.001	0.368
Probe: Bogota_BATALLON_BARAYA vs Bogota_AEROCIVIL	-2.465	0.016	[-2.497, -2.434]	<0.001	0.085
Probe: Bogota_BATALLON_USME vs Bogota_AEROCIVIL	-3.707	0.022	[-3.750, -3.665]	<0.001	0.025
Probe: Bogota_CAN_CGFM vs Bogota_AEROCIVIL	-2.505	0.016	[-2.537, -2.473]	<0.001	0.082
Probe: Bogota_MINTIC vs Bogota_AEROCIVIL	-2.09	0.02	[-2.129, -2.050]	<0.001	0.124
Probe: Bogota_TES_1 vs Bogota_AEROCIVIL	-4.048	0.03	[-4.106, -3.990]	<0.001	0.017

Reference categories: January, Monday and Bogota_AEROCIVIL. Abbreviations: Jan, Feb, Mar, Apr, May, Jun, Nov, Dec; Mon, Tue, Wed, Thu, Fri, Sat, Sun. Source: author's own elaboration.

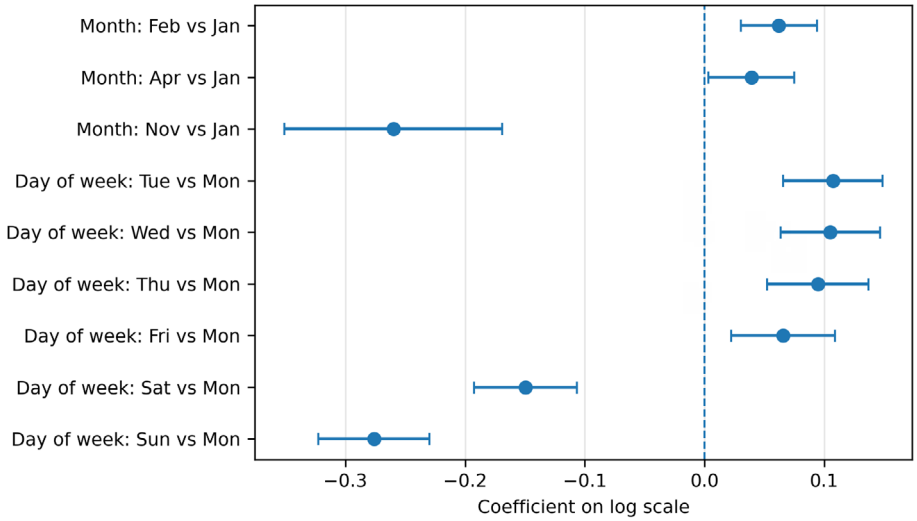

Fig. 4. *Selected temporal effects from the probe-adjusted model. Coefficients are shown on a logarithmic scale relative to January and Monday. Source: author's own elaboration.*

After adjusting for probe, the temporal effects became more stable and interpretable. Relative to January, February showed a

6.4% increase in mean daily exposure, April showed a 4.0% increase and November was 22.9% lower. Relative to Monday, higher values were observed from Tuesday to Friday, whereas Saturday and Sunday were lower. These effects are significant, but their magnitude is much smaller than that of the site coefficients.

Regression diagnostics, p95 robustness and robustness with mixed-effects models

The high adjusted R^2 of Model B required diagnostic verification. Table 5 shows that the residuals did not follow normality and that heteroscedasticity was present; therefore, HC3 robust standard errors were used for the inference of coefficients. The diagnostics also showed positive residual autocorrelation, with a pooled Durbin-Watson value of 0,598 and a median lag 1 residual autocorrelation per probe of 0,641. This autocorrelation implies that the exact temporal p-values should be interpreted with caution, especially for month effects. However, the influence diagnostics did not indicate that the fit was determined by a few high-leverage points: the maximum leverage was 0,0147, below the 2p/n threshold, and the maximum Cook's distance was 0,0278.

Table 5: Regression diagnostics for Model B.

Diagnostic	Result
Shapiro-Wilk residual normality	W = 0.926, p < 0.001
Jarque-Bera residual normality	JB = 3532.7, skew = -1.194, kurtosis = 9.041, p < 0.001
Breusch-Pagan heteroscedasticity	LM = 312.4, p < 0.001
Pooled Durbin-Watson	0.598
Median lag 1 residual ACF by probe	0.641
Range of lag 1 residual ACF by probe	0.222 to 0.936
Maximum leverage	0.0147
Leverage above 2p/n	0 observations (threshold = 0.0219)
Maximum Cook's distance	0.0278
Cook's distance above 4/n	98 observations (threshold = 0.0020)
Studentized residuals |r| > 3	23 of 2009 observations

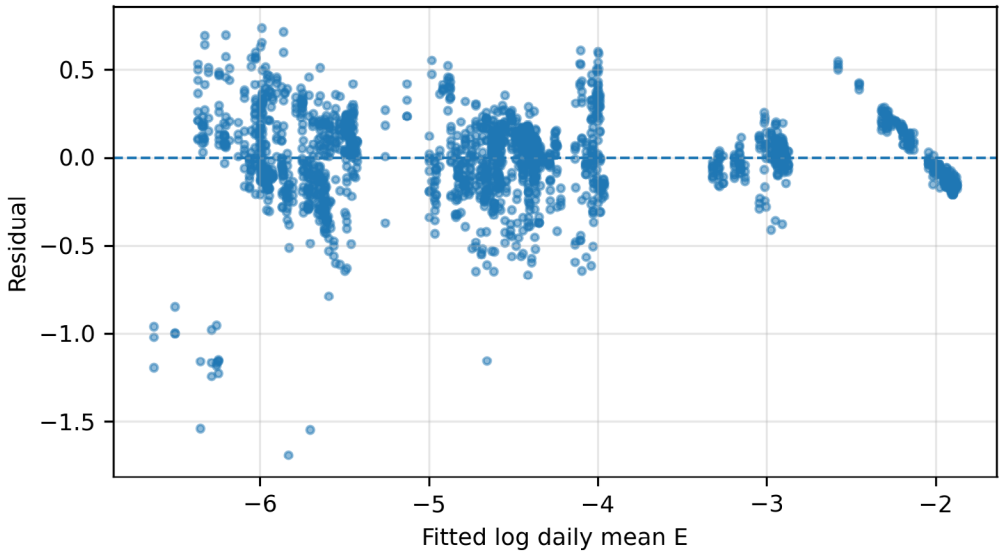

Fig. 5. *Residuals versus fitted values for Model B.*
The diagnostics qualify the inference and support the use of robust and panel-sensitive checks. Source: author's own elaboration.

The p95 model directly addressed the reviewer's concern about excluding the upper tail metric from the inferential analysis. The p95 model reached an adjusted R^2 of 0.951, and its coefficients preserved the same qualitative structure as the mean model: upper tail exposure remained dominated by persistent site differences, while day-of-week effects remained visible and weekends were lower. Table 6 shows selected p95 coefficients; the full p95 model table is exported by the revised R script.

The random-intercept mixed-effects model provided a second robustness check for the longitudinal structure. When the probe was modeled as a random intercept instead of fixed probe indicators, the marginal R^2 associated solely with temporal effects was 0.016, whereas the conditional R^2 including the probe structure was 0.964. This result is consistent with Model B and confirms that the dominant structure of the Bogotá dataset is the persistent difference between monitoring sites, rather than the month or the day of the week alone.

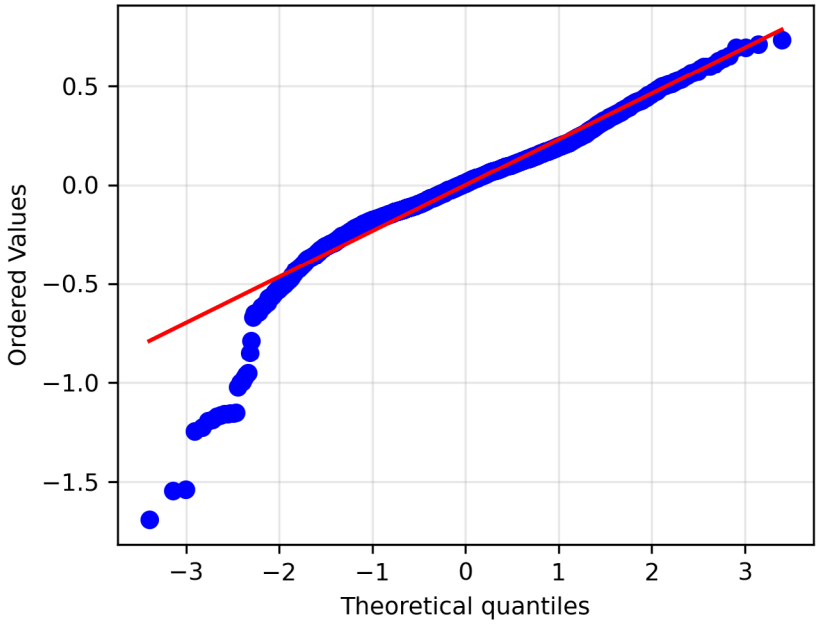

Fig. 6. *Q-Q plot of the residuals of Model B.*
Source: author's own elaboration.

Table 6: Selected coefficients of the complementary p95 model.

Term	Estimate	HC3 SE	IC 95%	p	Exp(beta)
Month: Feb vs Jan	0.07	0.02	[0.030, 0.109]	<0.001	1.072
Month: Apr vs Jan	0.079	0.023	[0.034, 0.123]	<0.001	1.082
Month: Nov vs Jan	-0.219	0.043	[-0.302, -0.135]	<0.001	0.804
Day: Tue vs Mon	0.149	0.025	[0.099, 0.199]	<0.001	1.161
Day: Sun vs Mon	-0.346	0.029	[-0.402, -0.289]	<0.001	0.708
Probe: Bogota_ANE_2 vs Bogota_AEROCIVIL	-0.629	0.017	[-0.663, -0.595]	<0.001	0.533
Probe: Bogota_MINTIC vs Bogota_AEROCIVIL	-1.671	0.026	[-1.723, -1.620]	<0.001	0.188
Probe: Bogota_TES_1 vs Bogota_AEROCIVIL	-3.908	0.029	[-3.965, -3.851]	<0.001	0.02

Response variable: daily log p95 of E. Reference categories: January, Monday and Bogota_AEROCIVIL. Source: author's own elaboration.

Technical interpretation of site and time effects

Bogota_AEROCIVIL was the site with the highest level in both the descriptive and adjusted analyses. Because the ANE release does not include metadata resolved by source or by frequency, this result should not be interpreted as a causal estimate of a specific transmitter or service. A non-causal technical explanation is that the site may be located in a denser radioelectric environment, potentially influenced by surrounding telecommunications infrastructure, aeronautical or institutional communications, rooftop or macrocell deployments, line-of-sight conditions and local urban propagation features. Broadband monitors integrate all active services within their measurement band, so a persistent elevation at a fixed probe is technically plausible even when absolute levels remain well below public reference values.

The sign reversal for November is also explained by site composition. In the raw monthly profile, November appears elevated because the early part of the dataset includes a strong contribution from higher-level probes, particularly Bogota_AEROCIVIL. Once the model holds the probe constant, November is no longer compared as a simple city average but is compared within the same site baseline. This is why the adjusted November coefficient becomes negative relative to January. This is not a contradiction, but an example of confounding between calendar effects and monitoring-site composition.

The pattern by day of the week is more stable. From Tuesday to Friday the values were higher than on Monday, whereas Saturday and Sunday were lower in both the mean and the p95 specifications. From an engineering perspective, this supports the interpretation that recurring weekly changes in aggregate network activity modulate the measured field. Even so, the much larger probe effects show that weekly modulation is secondary to persistent site conditions.

Engineering implications, limitations and data governance

Restricting the analysis to Bogotá changes the practical meaning of the results. The model does not compare heterogeneous cities, but rather multiple fixed monitors within the same metropolitan radioelectric environment. Therefore, site-specific baselines are more suitable than general city averages for establishing normal conditions, communicating expected ranges at

each probe, and identifying days that warrant follow-up.

Higher-level sites such as Bogota_AEROCIVIL and Bogota_ANE_2 are natural candidates for trend monitoring or targeted audits, not because they approach restrictive public limits, but because changes in the surrounding radioelectric environment are more likely to become detectable there. In contrast, lower-level probes offer useful reference contexts for anomaly detection and for public communication about how much exposure can vary within the same city while remaining low in absolute terms.

The inconsistency between the archived documentation of 28 V/m and the current Limite_Restrictivo and Porcentaje_Exposicion fields in the CSV reinforces the importance of modeling the measured variable directly in V/m instead of relying on derived percentage fields. Public monitoring datasets are analytically valuable only if the semantics of their variables are audited with the same care as the statistical procedure.

This study also has limitations. The released dataset does not provide metadata resolved by source, frequency, traffic, antenna or weather, so site effects should not be interpreted as causal estimates of specific transmitters or technologies. The window covers eight months, sufficient for short-term structure but not for multi-year evolution. Daily aggregation suppresses intraday dynamics, and residual autocorrelation suggests that future work should extend the workflow toward hourly models, generalized least squares, autoregressive structures, change-point analysis or frequency-resolved monitoring as richer releases become available, especially under 5G deployment scenarios[24],[25].

CONCLUSIONS

This study reorganized the ANE open monitoring dataset around a single metropolitan case: Bogotá. From 481,148 six-minute broadband measurements collected by nine fixed probes, the workflow constructed 2,009 nearly complete probe-day records and used them to characterize exposure levels, compare temporal and site-adjusted models, evaluate diagnostics, and verify robustness using p95 and mixed-effects models.

The descriptive results showed that field levels in Bogotá remained low in absolute terms. The highest six-minute value observed was 0.21011 V/m, still below 1% of the contextual public reference of 28 V/m described in the archived documentation. At the same time, the city exhibited pronounced heterogeneity across sites, with Bogota_AEROCIVIL and Bogota_ANE_2 consistently occupying the upper end of the distribution.

The modeling results refined that interpretation. A temporal-only model explained almost no variation, whereas the probe-adjusted model explained most of it. Diagnostics showed heteroscedasticity, non-normality, and residual autocorrelation, but the high fit was not produced by high-leverage observations. The p95 model and the random-intercept mixed-effects model supported the same conclusion: temporal variation exists, but site-specific persistent behavior is the dominant structure of the Bogotá dataset.

The main contribution is therefore methodological and operational. Open continuous monitoring data can support interpretable, site-sensitive analyses when preprocessing rules are explicit, variable semantics are audited, complete model outputs are reported, and upper-tail behavior is verified. For Bogotá, the results support probe-level baselines for comparison, anomaly detection, and public technical communication. The revised R workflow can be reused for future ANE releases or extended to richer monitoring contexts when additional metadata become available.

REFERENCES

[1] World Health Organization, “Electromagnetic fields,” WHO Health Topics. [Online]. Available: https://www.who.int/health-topics/electromagnetic-fields (accessed Apr. 2025).

[2] World Health Organization, “Radiation: Electromagnetic fields,” WHO Questions and Answers. [Online]. Available: https://www.who.int/news-room/questions-and-answers/item/radiation-electromagnetic-fields (accessed Apr. 2025).

[3] International Telecommunication Union, “Recommendation ITU-T K.83: Monitoring of electromagnetic field levels,” ITU-T, Geneva, Switzerland, Aug. 2024. [Online]. Available: https://www.itu.int/rec/T-REC-K.83-202408-I

[4] Agencia Nacional del Espectro, “Resolución 774 de 2018 por la cual se establecen los límites de exposición de las personas a los campos electromagnéticos,” ANE, Bogotá, Colombia, 2018. [Online]. Available: https://www.ane.gov.co/Documentos%20compartidos/ArchivosDescargables/Normatividad/Radiaciones_no_ionizantes/Resol_774-2018.pdf

[5] Agencia Nacional del Espectro, “Mediciones de exposición a campos electromagnéticos del sistema de monitoreo de campos electromagnéticos: Documento soporte datos abiertos,” ANE, Bogotá, Colombia, 2020. [Online]. Available: https://www.ane.gov.co/Documentos%20compartidos/ArchivosDescargables/datos-abiertos/Documento%20Soporte%20Datos%20Abiertos.pdf

[6] International Commission on Non-Ionizing Radiation Protection, “Guidelines for limiting exposure to electromagnetic fields (100 kHz to 300 GHz),” *Health Phys.*, vol. 118, no. 5, pp. 483–524, May 2020, doi: 10.1097/HP.0000000000001210.

[7] G. Dürrenberger, J. Fröhlich, M. Röösli, and M.-O. Mattsson, “EMF monitoring—concepts, activities, gaps and options,” *Int. J. Environ. Res. Public Health*, vol. 11, no. 9, pp. 9460–9479, Sep. 2014, doi: 10.3390/ijerph110909460.

[8] S. Sagar, S. Dongus, A. Schoeni, K. Roser, M. Eeftens, B. Struchen, M. Foerster, N. Meier, S. Adem, and M. Röösli, "Radiofrequency electromagnetic field exposure in everyday microenvironments in Europe: A systematic literature review," *J. Expo. Sci. Environ. Epidemiol.*, vol. 28, no. 2, pp. 147–160, Mar. 2018, doi: 10.1038/jes.2017.13.

[9] H. Jalilian, M. Eeftens, M. Ziaei, and M. Röösli, "Public exposure to radiofrequency electromagnetic fields in everyday microenvironments: An updated systematic review for Europe," *Environ. Res.*, vol. 176, art. no. 108517, Sep. 2019, doi: 10.1016/j.envres.2019.05.048.

[10] A. Manassas, A. Boursianis, T. Samaras, and J. N. Sahalos, "Continuous electromagnetic radiation monitoring in the environment: Analysis of the results in Greece," *Radiat. Prot. Dosimetry*, vol. 151, no. 3, pp. 437–442, Sep. 2012, doi: 10.1093/rpd/ncs028.

[11] I. Karastergios, A. Gialofas, and E. Karabetsos, "National observatory of electromagnetic fields: National telemetric network for the measurement of high-frequency electromagnetic fields in Greece," *Radiat. Prot. Dosimetry*, vol. 188, no. 4, pp. 413–423, Jul. 2020, doi: 10.1093/rpd/ncz301.

[12] A. Manassas, C. Apostolidis, S. Iakovidis, D. Babas, and T. Samaras, "A study of the long term changes in the electromagnetic environment using data from continuous monitoring sensors in Greece," *Sci. Rep.*, vol. 13, art. no. 13784, Aug. 2023, doi: 10.1038/s41598-023-41034-3.

[13] P. A. Valberg, T. E. van Deventer, and M. H. Repacholi, "Workgroup report: Base stations and wireless networks—radiofrequency (RF) exposures and health consequences," *Environ. Health Perspect.*, vol. 115, no. 3, pp. 416–424, Mar. 2007, doi: 10.1289/ehp.9633.

[14] P. Frei, E. Mohler, G. Neubauer, G. Theis, A. Bürgi, J. Fröhlich, C. Braun-Fahrländer, J. Bolte, M. Egger, and M. Röösli, "Temporal and spatial variability of personal exposure to radio frequency electromagnetic fields," *Environ. Res.*, vol. 109, no. 6, pp. 779–785, Aug. 2009, doi: 10.1016/j.envres.2009.04.015.

[15] W. Joseph et al., "Comparison of personal radio frequency electromagnetic field exposure in different urban areas across Europe," *Environ. Res.*, vol. 110, no. 7, pp. 658–663, Oct. 2010, doi: 10.1016/j.envres.2010.06.009.

[16] A. Bürgi, D. Scanferla, and H. Lehmann, "A model for radiofrequency electromagnetic field predictions at outdoor and indoor locations in the context of epidemiological research," *Bioelectromagnetics*, vol. 31, no. 3, pp. 226–236, Apr. 2010, doi: 10.1002/bem.20552.

[17] S. Aerts et al., "Exposure assessment of mobile phone base station radiation in an outdoor environment using sequential surrogate modeling," *Bioelectromagnetics*, vol. 34, no. 4, pp. 300–311, May 2013, doi: 10.1002/bem.21764.

[18] J. Beekhuizen, R. Vermeulen, H. Kromhout, A. Bürgi, and A. Huss, "Geospatial modelling of electromagnetic fields from mobile phone base stations," Sci. Total Environ., vols. 445–446, pp. 202–209, Feb. 2013, doi: 10.1016/j.scitotenv.2012.12.020.

[19] D. Urbinello, W. Joseph, L. Verloock, L. Martens, and M. Röösli, "Temporal trends of radio-frequency electromagnetic field exposure in everyday environments across European cities," *Environ. Res.*, vol. 134, pp. 134–142, Oct. 2014, doi: 10.1016/j.envres.2014.07.003.

[20] S. Aerts, W. Joseph, D. Deschrijver, L. Verloock, T. Dhaene, and L. Martens, "Assessment of long-term spatio-temporal radiofrequency electromagnetic field exposure," *Environ. Res.*, vol. 161, pp. 136–143, Feb. 2018, doi: 10.1016/j.envres.2017.11.003.

[21] S. Sagar et al., "Comparison of radiofrequency electromagnetic field exposure levels in different everyday microenvironments in an international context," *Environ. Int.*, vol. 114, pp. 297–306, May 2018, doi: 10.1016/j.envint.2018.02.036.

[22] R Core Team, "R: A Language and Environment for Statistical Computing," R Foundation for Statistical Computing, Vienna, Austria, 2024. [Online]. Available: https://www.R-project.org/.

[23] M. J. van Wyk, J. C. Visser, and C. W. le Roux, "Measurement of EMF exposure around small cell base station sites," *Radiat. Prot. Dosimetry*, vol. 184, no. 2, pp. 211–215, Aug. 2019, doi: 10.1093/rpd/ncy201.

[24] S. Aerts et al., "RF-EMF exposure near 5G NR small cells," *Sensors*, vol. 23, no. 6, art. no. 3145, Mar. 2023, doi: 10.3390/s23063145.

[25] S. Liu, K. Tobita, T. Onishi, M. Taki, and S. Watanabe, "Electromagnetic field exposure monitoring of commercial 28-GHz band 5G base stations in Tokyo, Japan," *Bioelectromagnetics*, vol. 45, no. 6, pp. 281–292, Sep. 2024, doi: 10.1002/bem.22505.

[26] J. C. Pinheiro and D. M. Bates, Mixed-Effects Models in S and S-PLUS. New York, NY, USA: Springer, 2000.

[27] J. M. Wooldridge, Econometric Analysis of Cross Section and Panel Data, 2nd ed. Cambridge, MA, USA: MIT Press, 2010.

[28] J. Fox and S. Weisberg, An R Companion to Applied Regression, 3rd ed. Thousand Oaks, CA, USA: Sage, 2019.

DECLARATION OF ARTIFICIAL INTELLIGENCE USE

During the review of this manuscript, a generative artificial intelligence assistant was used as support for language editing, translation, document organization, and preparation of responses to reviewers. The numerical results were generated from the provided dataset using auditable code and were reviewed by the authors. The authors assume full responsibility for the final content, interpretation, and conclusions of this publication.

ACKNOWLEDGMENTS

The authors thank the National Spectrum Agency for publishing the continuous monitoring dataset used in this study.

FUNDING

This research received no external funding.

CONFLICT OF INTEREST

None

AUTHORSHIP CONTRIBUTIONS

Following the CRediT (Contributor Roles Taxonomy) framework, the contributions of each author were: Conceptualization: O.B.-C., J.G.P.-H., and C.D.C.-A.; data curation: O.B.-C. and C.D.C.-A.; formal analysis: O.B.-C. and C.D.C.-A.; funding: none; investigation: O.B.-C., J.G.P.-H., and C.D.C.-A.; methodology: O.B.-C., J.G.P.-H., and C.D.C.-A.; project administration: O.B.-C., J.G.P.-H., and C.D.C.-A.; resources: O.B.-C.; software: O.B.-C., J.G.P.-H., and C.D.C.-A.; supervision: O.B.-C., J.G.P.-H., and C.D.C.-A.; validation: O.B.-C., J.G.P.-H., and C.D.C.-A.; visualization: O.B.-C.; writing—original draft: O.B.-C., J.G.P.-H., and C.D.C.-A.; writing—review and editing: O.B.-C., J.G.P.-H., and C.D.C.-A. All authors read and approved the final version of the manuscript.